

# Growth and structure of TiC coatings chemically vapour deposited on graphite substrates

S. EROGLU\*, B. GALLOIS

*Stevens Institute of Technology, Department of Materials Science and Engineering, Hoboken, NJ 07030, USA*

TiC coatings were grown on graphite substrates by the chemical vapour deposition technique, using gas mixtures of  $\text{CH}_4$ – $\text{TiCl}_4$ – $\text{H}_2$  at a total pressure of 10.7 kPa and at temperatures of 1400 and 1425 K. The growth rate and structure of the TiC coatings were investigated as a function of  $\text{CH}_4$  and  $\text{H}_2$  concentrations. The deposition rate of TiC increased with increasing  $\text{CH}_4$  flow rate, but did not change with  $\text{H}_2$  flow rate. This behaviour was explained by a mass transport theory. Thermodynamic analyses based on minimization of Gibbs' free energy predicted carbon codeposition with TiC. X-ray diffraction and Auger electron spectroscopy (AES) studies and microstructural observations, however, suggested that free carbon did not form. Textural analyses indicated that the growth of TiC coatings was initiated as randomly oriented crystallites, and as the thickness of the coatings increased, preferentially oriented columnar grains developed. The textures of TiC coatings with the same thickness changed from the  $\langle 110 \rangle$  orientation to the  $\langle 100 \rangle$  orientation with decreasing  $\text{H}_2$  flow rate for a constant  $\text{CH}_4$  flow rate. The  $\text{CH}_4$  concentration also greatly influenced the preferred orientation of the coatings.

## 1. Introduction

Titanium carbide (TiC) coatings have high hardness, high temperature strength and good corrosion resistance; because of these properties, they have been used in many areas, ranging from cutting tools to nuclear materials. The use of protective TiC coatings is an effective method to improve the surface characteristics of graphite and graphite based materials. For example, TiC coatings deposited on graphite substrates as used in fusion reactors reduce surface erosion and help to improve plasma impurity control [1, 2].

The chemical vapour deposition (CVD) technique has been widely used to prepare TiC coatings. TiC coatings deposited on metals (Mo, steel, Fe) or cemented carbide (WC–Co) substrates by this technique have been the subject of extensive research. Although a number of studies [3, 4] have investigated the chemical vapour deposition of TiC on graphite substrates using  $\text{CH}_4$  gas as a carbon source, there is little information concerning the effect of CVD parameters on the growth rate, composition and texture of the TiC coatings. Klein and Gallois [5] investigated the early growth of TiC coatings on a graphite substrate. The effect of deposition temperature on the deposition rate and morphology of TiC has been reported by Paik [6]. This study was undertaken in order to investigate systematically the influence of input gas composition on the growth rate,

composition and texture of the TiC coatings grown on graphite substrates.

### 1.1. Equilibrium thermodynamic analysis

Thermodynamic calculations based on the minimization of the Gibbs' free energy were performed for input gas mixtures of  $\text{TiCl}_4$ ,  $\text{CH}_4$  and  $\text{H}_2$  at 1400 K. The principles of the thermodynamic approach are described elsewhere [7]. For a system of known initial gas composition, this method gives both the vapour phase and deposit compositions at a given temperature and pressure when equilibrium is reached. The calculations require specifying all possible species and condensed phases which can exist in the temperature range of interest. In the Ti–Cl–C–H system, 44 gaseous species can be considered as constituents of the gas phase. They include  $\text{TiCl}_4$ ,  $\text{TiCl}_3$ ,  $\text{TiCl}_2$ ,  $\text{TiCl}$ ,  $\text{CH}_4$ ,  $\text{C}_2\text{H}_2$ ,  $\text{C}_2\text{H}_3$ ,  $\text{CH}_3\text{Cl}$ ,  $\text{HCl}$ ,  $\text{Cl}_2$  and  $\text{H}_2$ .  $\beta$ -titanium, C and stoichiometric TiC are the possible solid equilibrium phases. Thermodynamic data for the species were taken from the JANAF tables [8].

Fig. 1 shows the CVD phase diagram of the Ti–Cl–C–H system as a function of initial partial pressures of  $\text{TiCl}_4$  and  $\text{CH}_4$  at a constant temperature of 1400 K and a total pressure of 10 kPa. Hydrogen makes up the difference between 10 kPa and the sum of the partial pressures of  $\text{TiCl}_4$  and  $\text{CH}_4$ . The diagram is dominated by the phase fields of TiC and

\* Present address: TUBITAK, Marmara Research Center, Materials Research Division, Gebze-Kocaeli, Turkey.

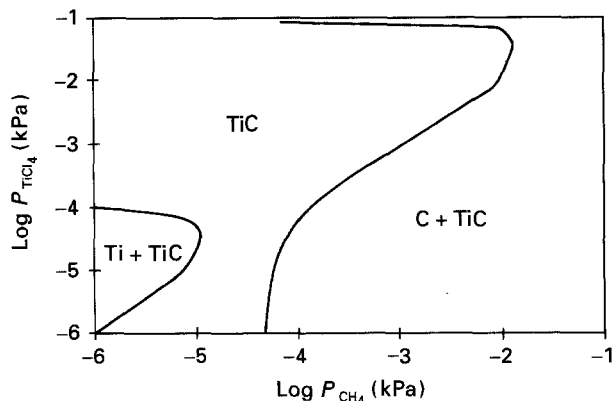


Figure 1 CVD phase diagram showing the condensed phases which deposit at equilibrium as a function of partial pressures of  $\text{TiCl}_4$  and  $\text{CH}_4$  for the Ti-Cl-C-H system at 1400 K and a total pressure of 10 kPa. The total pressure is maintained constant with hydrogen.

TiC + C in the partial pressure range of interest. Titanium carbide is deposited at equilibrium as a single phase under a wide range of initial compositions. The deposition range of TiC increases with increasing partial pressures of  $\text{CH}_4$  and  $\text{TiCl}_4$ . It is not codeposited with carbon at low partial pressures of  $\text{CH}_4$ . The Ti + TiC phase field is very narrow and limited to low partial pressures of  $\text{TiCl}_4$  and  $\text{CH}_4$ , with the partial pressure of  $\text{TiCl}_4$  larger than that of  $\text{CH}_4$ . Thermodynamic calculations indicate that for molar ratios of  $\text{CH}_4/\text{TiCl}_4$  larger than unity, free carbon is codeposited with TiC, in increasing amount with the increase in C/Ti ratio in the gas phase.

## 2. Experimental details

### 2.1. Chemical vapour deposition

The deposition experiments were carried out in a computer controlled hot wall chemical vapour deposition reactor. A detailed description of the reactor is given by Paik [6]. The substrates were rectangles  $2 \times 1$  cm, 1 mm thick, cut from graphite materials whose properties are tabulated elsewhere [9]. The CVD experiments were conducted at a total pressure of 10.7 kPa, a total flow rate of 670 standard cubic centimeters per minute (sccm) and temperatures of 1400 and 1425 K. At these temperatures, the growth of the TiC coatings has been reported to be controlled by mass transport of the gaseous species from the gas phase to the surface of deposit [6]. The experimental deposition conditions employed for the chemical vapour deposition of the TiC coatings are shown in Table I. The experiments were divided into three series at 1425 K. In the first series, the flow rate of hydrogen was varied from 100 to 600 sccm at constant  $\text{CH}_4$  (50 sccm) and  $\text{TiCl}_4$  (20 sccm) flow rates. The total flow rate was maintained constant with argon. The purpose of these experiments was to investigate the effect of hydrogen concentration on the deposition rate and the crystallographic texture of the coatings. In the second series, the effect of methane concentration was investigated by varying the flow rate of methane from 0 to 360 sccm at a constant  $\text{TiCl}_4$  flow rate of 20 sccm. Finally two experiments were performed at a  $\text{TiCl}_4$  flow rate of 10 sccm and  $\text{CH}_4$  flow rates of 260

TABLE I Experimental conditions for the chemical vapour deposition of TiC coatings

Deposition temperature (K)	Flow rate (sccm)				Growth rate ( $\mu\text{m min}^{-1}$ )
	$\text{TiCl}_4$	$\text{CH}_4$	$\text{H}_2$	Ar	
1425, Series I	20	50	100	500	$0.104 \pm 0.009$
	20	50	200	400	$0.119 \pm 0.007$
	20	50	300	300	$0.093 \pm 0.003$
	20	50	400	200	$0.107 \pm 0.005$
	20	50	500	100	$0.106 \pm 0.005$
	20	50	600	—	0.109
1425, Series II	20	—	650	—	0.017
	20	50	600	—	0.110
	20	70	580	—	0.130
	20	160	490	—	$0.170 \pm 0.01$
	20	210	440	—	$0.370 \pm 0.01$
	20	260	390	—	$0.400 \pm 0.03$
	20	310	340	—	$0.540 \pm 0.01$
	20	360	290	—	$0.780 \pm 0.03$
1425, Series III	10	260	400	—	<sup>a</sup>
	10	360	300	—	<sup>a</sup>
1400	20	—	650	—	0.017
	20	50	600	—	0.075
	20	175	475	—	$0.231 \pm 0.001$
	20	370	280	—	$0.543 \pm 0.06$

<sup>a</sup> Powdery deposits.

and 360 sccm. At 1400 K, the effect of  $\text{CH}_4$  concentration on the growth rate of the TiC coatings was also investigated.

### 2.2. Characterization

#### 2.2.1. Scanning electron microscopy and Auger electron spectroscopy

The morphology of the coatings was examined in a Jeol scanning electron microscope (model JSM-840). Samples were coated with a thin layer of gold by sputtering from a gold target at 70 mA for 10 s. The thickness of the coatings was determined from micrographs of cross-sections.

Auger electron spectroscopy was performed on the TiC coatings in order to study their composition. The electron beam energy was 3 keV with a 0.005  $\mu\text{A}$  beam current. The diameter of the electron beam was equal to 20  $\mu\text{m}$ .

#### 2.2.2. X-ray diffraction (XRD)

Precise lattice parameter measurements were performed on a General Electric XRD-6 parafocusing diffractometer equipped with a copper tube and  $\text{NiK}_\beta$  filter. The alignment of the diffractometer was checked by measuring the lattice constant of a stress-free powdered silicon sample. Lattice parameters of TiC coatings were measured using the  $\text{K}_{\alpha_1}$  and  $\text{K}_{\alpha_2}$  reflections of the (1 1 5), (2 2 4), (4 2 0) and (3 3 1) crystal planes. The peak position was determined by fitting a parabola to the top part of the profile, after the corrections for Lorentz polarization factors. The Nelson-Riley analysis [10] was then applied to obtain the true lattice parameter.

Preferred orientation, expressed in terms of texture coefficients, was determined with the parafocusing diffractometer. The reflections from the (111), (200), (220) and (113) crystal planes were used to investigate textures in the coatings. The relative integrated intensities of the peaks were determined by measuring the area of each peak above background, and normalizing the areas with respect to the highest intensity peak. The intensity data were analysed by the Harris method [10]. The method calculates texture coefficient (TC), the fraction of grains having any particular  $\{hkl\}$  plane parallel to the surface

$$TC_{hkl} = \frac{I_{hkl}/I_{hkl}^0}{(1/n)\Sigma(I_{hkl}/I_{hkl}^0)} \quad (1)$$

where  $I_{hkl}$  and  $I_{hkl}^0$  are the integrated intensities of the coating and powdered TiC, respectively, and  $n$  is the number of reflections used. Data for randomly oriented TiC were obtained from the JCPDS powder file [11].

### 3. Results and discussion

#### 3.1. Deposition rates

The growth rate of TiC coatings at 1400 and 1425 K was investigated as a function of CH<sub>4</sub> flow rate. As shown in the Fig. 2a, the deposition rate of TiC grown at 1400 K linearly increases with CH<sub>4</sub> concentration in the gas phase. A slight deviation from linear dependence of the growth rate on CH<sub>4</sub> flow rate was observed at 1425 K (Fig. 2b). It should be noted that TiC coatings were grown without CH<sub>4</sub> due to the carbon supply from the graphite substrates. The increase in growth rate with CH<sub>4</sub> flow rate can be explained as follows: since deposition was carried out in the mass transport limited regime, the deposition process was controlled by mass transport of gas species from the bulk gas phase to the surface. An important feature of the chemical vapour deposition process is the presence of a boundary layer just above the substrate [12]. In this regime, the deposition rate is proportional to the mass transport flux of gaseous reactants through the boundary layer, which is given by [13]

$$J_i = -h_g(C_b - C_s) \quad (2)$$

where  $J_i$  is the mass transport flux of species  $i$ ,  $h_g$  is the mass transport coefficient of species  $i$ ,  $C_b$  is the bulk gas concentration, and  $C_s$  is the surface concentration. The mass transport coefficient is given by [13]

$$h_g = D_g/\delta \quad (3)$$

where  $D_g$  is the diffusion coefficient and  $\delta$  is the boundary layer thickness above the substrate. The diffusion coefficient [14] is given by

$$D_g \propto T^{3/2}/P \quad (4)$$

where  $T$  is the deposition temperature and  $P$  is the total pressure. The thickness of boundary layer is given by [13]

$$\delta \propto (\mu/v)^{1/2} \quad (5)$$

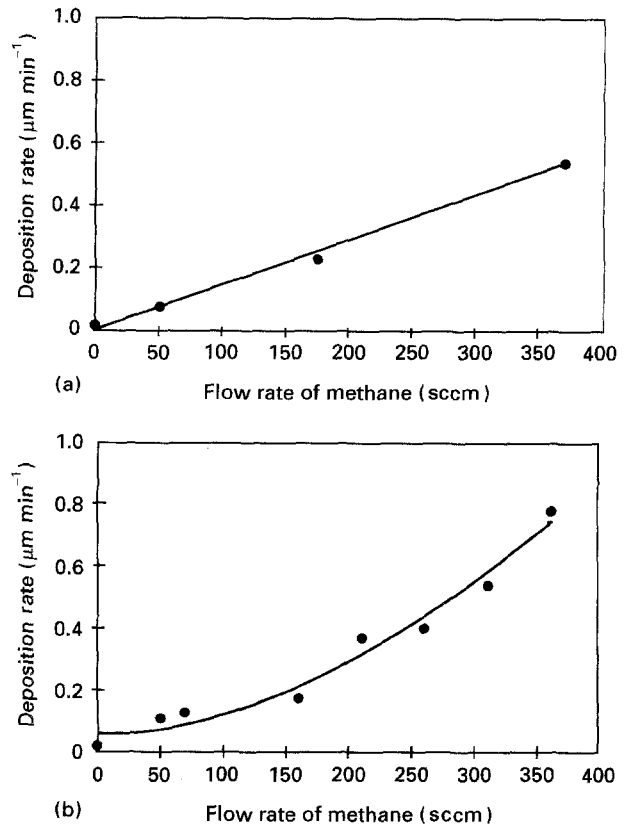


Figure 2 Variation of deposition rate as a function of CH<sub>4</sub> flow rate at (a) 1400 and (b) 1425 K. The flow rate of TiCl<sub>4</sub> is 20 sccm. Total flow rate of 670 sccm is maintained constant with H<sub>2</sub>.

where  $\mu$  is the kinematic viscosity and  $v$  is the linear gas velocity. Substituting Equations 3–5 into Equation 2, the deposition rate can be expressed as

$$\text{rate} \propto (T^{3/2}/P)(v/\mu)^{1/2}(C_b - C_s) \quad (6)$$

Since the deposition temperature, the total pressure and the total flow rate were held constant, the rate is proportional to the concentration potential across the boundary layer, assuming no change in kinematic viscosity with gas composition. In the mass transport controlled regime, the diffusion process by which reactant compounds are transported to the growth surface proceeds much slower than reactant consumption by the actual growth reaction on the deposition surface. Therefore, it may be assumed that  $C_b$  is much larger than  $C_s$ . Equation 6 then becomes

$$\text{rate} \propto C_b \quad (7)$$

Equation 7 indicates that the growth rate of titanium carbide is linearly proportional to the reactant concentration. Since hydrogen does not affect the growth rate of TiC, as shown in Table I, and titanium tetrachloride is constant, the deposition rate should increase linearly with the concentration or flow rate of methane. This behaviour is in fairly good agreement with the experimental results (Fig. 2).

The coatings deposited at CH<sub>4</sub>/TiCl<sub>4</sub> ratios of 26 and 36 were powdery because of homogeneous gas phase reactions.

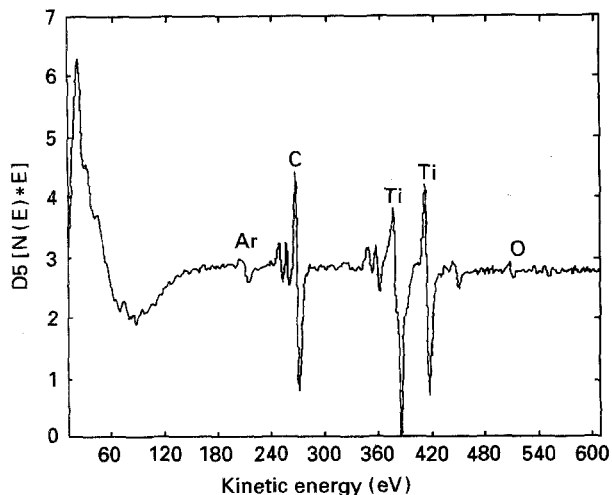


Figure 3 A typical Auger spectrum from TiC coatings grown at 1425 K and a  $\text{CH}_4/\text{TiCl}_4$  ratio of 18. The spectrum was taken after sputtering for 20 min with  $\text{Ar}^+$  ions at 3 keV.

### 3.2. Compositional analysis

Auger electron spectroscopy (AES) was performed on the TiC coatings in order to study their compositions. Sundgren *et al.* [15] reported that the appearance of free carbon in over-stoichiometric titanium carbide coatings is signalled by characteristic changes in the C (272 eV) peak. The intensity of the positive excursion of the carbon peak is much smaller than that of the negative excursion for the over-stoichiometric titanium carbide, whereas stoichiometric TiC has almost the same intensities for the negative and positive excursions. Fig. 3 shows an Auger spectrum of the coating grown at a  $\text{CH}_4$  flow rate of 360 sccm. The shape of the carbon peak is typical of titanium carbide for all gas compositions. It is also observed that the ratio of the carbon peak (272 eV) to the titanium peak (418 eV) does not change with gas composition. Due to the lack of a standard TiC sample, no quantification of Auger results was attempted. The measured peak ratio was, however, compared with the literature values determined for stoichiometric TiC. It was found that the experimental ratio of  $1.04 \pm 0.04$  (the average for all coatings) was close to published values for stoichiometric TiC, which range from 0.95 to 1.07 [16–18]. This result suggests that the coatings were stoichiometric.

In order to determine the effect of the  $\text{CH}_4/\text{TiCl}_4$  ratio in the gas phase on the compositions of the coatings, lattice parameters were measured by X-ray diffraction techniques. The average of the lattice parameters was calculated to be 0.43270 nm, with a standard deviation of 0.00004 nm, indicating that the lattice constant does not change with the  $\text{CH}_4/\text{TiCl}_4$  ratio. It is known [19] that the lattice parameter of  $\text{TiC}_x$  does not linearly depend on carbon content,  $x$ , in the compound. The lattice parameter increases with  $x$  below 0.85, at which point a maximum is reached ( $a = 0.433$  nm) and then decreases above 0.85. The results on the basis of lattice parameter calculations indicate that the coatings of TiC may be stoichiometric. No free carbon was detected by X-ray diffraction.

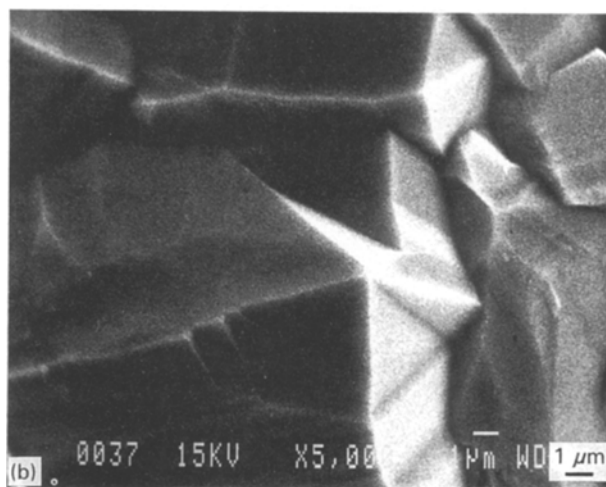
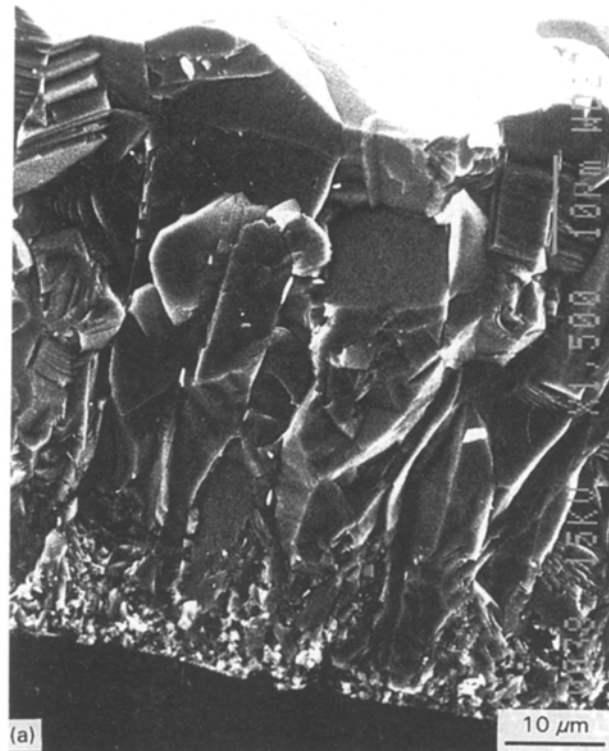


Figure 4 Scanning electron micrographs of the TiC coating grown at 1425 K and at a  $\text{CH}_4$  flow rate of 360 sccm: (a) cross-sectional view and (b) surface morphology.

It is known that deposition of a second phase leads to grain refinement in chemically vapour deposited coatings. Fig. 4a, b shows the cross-sectional view and surface morphology of the coating grown at a  $\text{CH}_4$  flow rate of 360 sccm. The coating exhibited columnar grains originating from small grains near the interface between the coating and the substrate and increasing in diameter with thickness. The surface morphology of the coating consisted of very large pyramidal grains, indicating that there was no evidence of grain refinement. This observation supports the conclusion that the coatings consisted of single phase TiC.

The thermodynamic calculations showing free carbon codeposited with TiC are in disagreement with the results of the experiments. This discrepancy suggests that the CVD process occurred under non-equilibrium

conditions. A kinetically limiting step in the pyrolysis of  $\text{CH}_4$  in the gas phase may be the cause of the absence of free carbon in the deposits.

### 3.3. Analysis of textures

X-ray diffraction analyses revealed that almost all coatings exhibited X-ray peak intensities which deviated from those observed in random powder samples. The coatings have a preferred orientation of a particular set of crystal planes parallel to the substrate, producing fibre texture with the fibre axis parallel to the growth direction. Fig. 5 shows the variation of the texture coefficients of the (111), (200), (220) and (113) reflections with coating thickness for coatings grown at 1400 K and at a  $\text{CH}_4$  flow rate of 50 sccm. As can be seen from the figure, the texture coefficient of the (220) crystal plane increases with coating thickness, while those of the (111), (200) and (113) planes are suppressed. The number of grains that have a  $\langle 110 \rangle$  growth orientation parallel to the growth direction increases. Texture studies indicate that the coatings at the beginning of the growth tend to have a nearly random structure, and a  $\langle 110 \rangle$  preferential growth orientation develops as growth proceeds. This

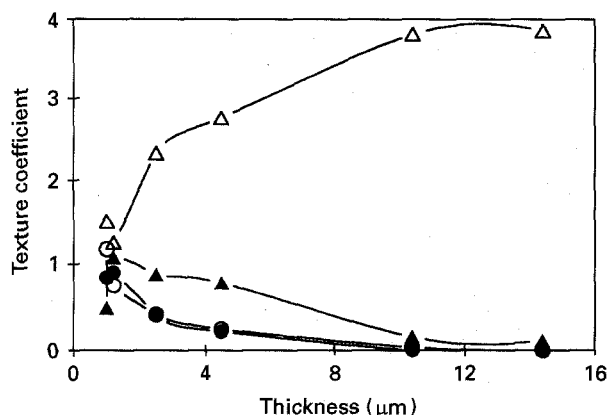


Figure 5 Variation of texture coefficients as a function of thickness for the coatings grown at 1400 K and at a  $\text{CH}_4$  flow rate of 50 sccm. Hydrogen flow rate was 600 sccm:  $\circ$ , (111);  $\bullet$ , (200);  $\triangle$ , (220); and  $\blacktriangle$ , (113).

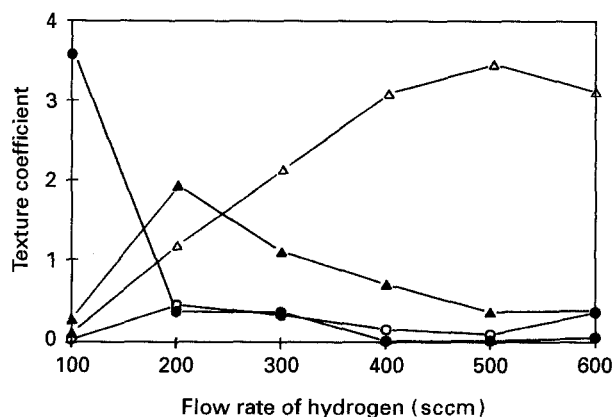


Figure 6 The effect of the flow rate of hydrogen on the preferred orientation of TiC coatings grown at a  $\text{CH}_4$  flow rate of 50 sccm and at 1425 K. The flow rate of 670 sccm was maintained constant with argon:  $\circ$ , (111);  $\bullet$ , (200);  $\triangle$ , (220);  $\blacktriangle$ , (113).

behaviour can be explained by evolutionary selection theory [20]. As shown in Fig. 4a, initial layers of the coatings are composed of fine grains. With increasing thickness, certain individual grains become greater in diameter; screening and suppressing less favourable grains. From these observations, it can be concluded that there is competition between differently orientated grains. As growth proceeds, more and more grains are overgrown by adjacent crystals, and the number of grains extending to the surface decreases progressively. Only those crystals with a  $\langle 110 \rangle$  growth orientation perpendicular or nearly perpendicular to the substrate surface survive, whereas grains with other orientations are gradually buried.

The effect of hydrogen concentration on preferred orientation of the coatings grown at 1425 K and at  $\text{CH}_4$  flow rate of 50 sccm is shown in Fig. 6. The thickness of the coatings was kept constant at around 8  $\mu\text{m}$ . As can be seen from the figure, the texture coefficient of the (200) plane decreases with increasing hydrogen concentration up to 200 sccm at which point a slight  $\langle 113 \rangle$  preferred orientation was observed. Above that the coating has a high  $\langle 110 \rangle$  orientation.

Table II shows the effect of input gas concentration on the preferred orientation of the coatings. The

TABLE II The effect of input gas composition on the texture coefficient of TiC coatings

Temperature (K)	$\text{CH}_4/\text{TiCl}_4$	Thickness ( $\mu\text{m}$ )	Texture coefficient			
			(111)	(200)	(220)	(113)
1425	0	1.0	0.94	1.23	1.23	0.60
	2.5	3.0	0.45	0.70	1.68	1.17
	8.0	12.0	0	2.54	0.08	1.38
	10.50	27.0	0	3.13	0	0.87
	13.00	30.0	0	1.27	0.89	1.84
	15.50	40.0	0	0.99	1.90	0.11
	18.00	54.0	0	0.37	2.10	1.52
	26.00	<sup>a</sup>	0.79	1.34	1.06	0.80
	36.00	<sup>a</sup>	0.74	1.13	1.09	1.04
	1400	0	1.0	1.18	0.84	1.51
2.50		4.5	0.22	0.20	2.70	0.88
8.75		17.3	0	3.79	0.05	0.16
18.50		40.7	0.12	0.89	1.86	1.19

<sup>a</sup> Powdery deposit.

information obtained from the table can be summarized as follows: thin coatings and powdery coatings had a nearly random structure as expected. The  $\langle 110 \rangle$  preferred orientation was favoured at low  $\text{CH}_4/\text{TiCl}_4$  ratios (2.5) as well as at high ratios (15.5 and 18). The coatings grown at medium ratios (8–13) exhibited a  $\langle 100 \rangle$  preferred orientation. It is interesting to note that the texture coefficient of the (111) crystal plane became zero when the ratio was above 2.5.

#### 4. Conclusions

The growth rate of TiC coatings deposited on graphite substrates in a mass transport limited regime linearly increased with  $\text{CH}_4$  concentration in the gas phase, and this behaviour was explained by a mass transport theory. Contrary to thermodynamic predictions, X-ray and Auger studies and microstructural observations indicated that the coatings consisted of a single phase of stoichiometric TiC. The growth of TiC coatings at a  $\text{CH}_4/\text{TiCl}_4$  ratio of 2.5 was initiated by fine grains, which developed into columnar grains with a sharp  $\langle 110 \rangle$  preferred orientation as growth proceeded. The  $\langle 100 \rangle$  and  $\langle 110 \rangle$  preferred orientations in the TiC coatings of the same thickness grown at a  $\text{CH}_4/\text{TiCl}_4$  ratio of 2.5 were favoured by low and high hydrogen concentrations, respectively.

#### Acknowledgements

The authors gratefully acknowledge the partial support of the Army Research Office, Division of Materials Science, under contract DAAG29-85-K-0124, and the New Jersey Advanced Technology Center for Surface Engineered Materials. S. Eroglu would like to thank "The Ministry of Education of the Republic of Turkey" for a scholarship enabling him to study in the USA.

#### References

1. M. KOMINSKY, R. NIELSEN and P. ZSCHACK, *J. Vac. Sci. Technol.* **20** (1982) 1304.

2. R. A. LANGLEY, L. C. EMERSON, J. B. WHITLEY and A. W. MULLENDORE, *J. Nuclear Mater.* **93&94** (1980) 479.
3. J. Y. ROSSIGNOL, F. LANGLAIS and R. NASLAIN, in "Proceedings of the Ninth International Conference on CVD", edited by M. Robinson, C. H. J. van den Brekel, G. W. Cullen, J. M. Blocher, Jr and P. Rai-Choudhury (Electrochemical Society, Pennington, PA, 1984) p. 596.
4. L. AGGOUR, E. FITZER and J. SCHLICHTINHG, in "Proceedings of the Fifth International Conference on CVD", edited by J. M. Blocher, Jr, G. E. Vuillard and G. Wahl (Electrochemical Society, Pennington, PA, 1981) p. 142.
5. M. KLEIN and B. M. GALLOIS, in "Chemical Vapor Deposition of Refractory Metals and Ceramics", edited by T. M. Besmann and B. M. Gallois. Symposium Proceedings, Vol. 168, (Materials Research Society, Pittsburgh, PA, 1989) p. 93.
6. J. S. PAIK, PhD thesis, Stevens Institute of Technology, Hoboken, NJ (1991).
7. T. M. BESMANN, Report TM-5775, Oak Ridge National Laboratory, TN (1977).
8. D. R. STULL and H. PROPHET, "JANAF Thermochemical Tables", 2nd Edn, NSRDS-NBS 37 GPO, Washington, DC (1971).
9. S. EROGLU and B. GALLOIS, *J. de Physique IV*, **3(C3)** (1993) 155.
10. C. S. BARRET and T. B. MASSALSKI, "Structure of Metals", 3rd Edn (Pergamon Press, Oxford, 1980) p. 204.
11. Joint Committee on Powder Diffraction Standards, File No. 6-0614 (JCPDS Philadelphia, PA, 1967).
12. F. C. EVERSTEYN, P. J. W. SEVERIN, C. H. J. van den BREKEL and H. L. PEEK, *J. Electrochem. Soc.* **117** (1970) 925.
13. A. S. GROVE, "Physics and Technology of Semiconductor Devices" (Wiley, New York, 1969) pp. 13–16.
14. S. DUSHMAN, "Scientific Foundations of Vacuum Technique" (Wiley, New York, 1962) p. 77.
15. J. E. SUNDGREN, A. ROCKETT, J. E. GREENE and U. HELMERSSON, *J. Vac. Sci. Technol. A*, **4** (1986) 2770.
16. D. W. KIM, Y. J. PARK, J. G. LEE and J. S. CHUN, *Thin Solid Films* **165** (1988) 149.
17. J. E. SUNDGREN, B. O. JOHANNSSON and S. E. KARLSSON, *ibid.* **105** (1983) 353.
18. S. KOMIYA, N. UMEZU and T. NARUSAWA, *ibid.* **54** (1978) 51.
19. C. JIANG, T. GOTO and T. HIRAI, *J. Mater. Sci.* **25** (1990) 1086.
20. A. van der DRIFT, *Phillips Research Reports* **22** (1967) 267.

Received 31 January

and accepted 7 September 1994